Detection of artificially generated ULF waves by the FAST spacecraft and its application to the "tagging" of narrow flux tubes

D. M. Wright,[1] J. A. Davies,[1] T. K. Yeoman,[1] T. R Robinson,[1] S. R. Cash,[1] E. Kolesnikova,[1] M. Lester,[1] P. J. Chapman,[1] R. J. Strangeway,[2] R. B. Horne,[3] M. T. Rietveld,[4,5] and C. W. Carlson[6]

Received 13 May 2002; revised 14 October 2002; accepted 4 November 2002; published 26 February 2003.

[1] Recently, *Robinson et al.* [2000] presented a brief report on the artificial generation of ULF waves by high power ionospheric modification and their subsequent detection by the Fast Auroral Snapshot (FAST) spacecraft. The radio frequency "heating" facility at Tromsø was employed to impose a 3-Hz modulation on the current system that constitutes the auroral electrojet, resulting in the injection of field-guided ULF waves into the magnetosphere. The electric and magnetic field signatures of the waves were detected directly by the FAST spacecraft. Furthermore, a signature in the downgoing field-aligned electron flux, also observed by the satellite, was postulated to have resulted from the interaction of the ULF waves with the upper boundary of the ionospheric Alfvén resonator. This paper evaluates these results in the context of the prevailing ionospheric conditions during the experiment and discusses the significance of the substorm activity, which occurred during this interval. The technique of artificial ULF wave injection, which can be used to "tag" narrow flux tubes, could play an important part in overcoming mapping issues between ground-based and space-based observations of phenomena that couple the ionosphere and magnetosphere. *INDEX TERMS:* 2752 Magnetospheric Physics: MHD waves and instabilities; 2403 Ionosphere: Active experiments; 2704 Magnetospheric Physics: Auroral phenomena (2407); 0694 Electromagnetics: Instrumentation and techniques; 2451 Ionosphere: Particle acceleration; *KEYWORDS:* high power RF heating, ULF waves, FAST spacecraft, ionospheric Alfven resonator

Citation: Wright, D. M., et al., Detection of artificially generated ULF waves by the FAST spacecraft and its application to the "tagging" of narrow flux tubes, *J. Geophys. Res.*, *108*(A2), 1090, doi:10.1029/2002JA009483, 2003.

1. Introduction

[2] An ever-increasing number of Earth-orbiting spacecraft provide many opportunities to compare magnetospheric phenomena with their signatures in the ionosphere and even at the ground. It is, therefore, important to be able to accurately map the locations of associated features along field lines from the Earth into space and vice versa. Normally, long established magnetic field models such as the International Geomagnetic Reference Field (IGRF) [e.g., *Barton et al.*, 1996] are employed for this purpose. However, these are only average fields and adjustments are often necessary using measurements from ground magnetometers on a case by case basis. The ability to "tag" the field lines which spacecraft are traversing would be of great value to those wishing to identify relatively localized structures or flux tubes as well as time dependent transient processes common to both spacecraft data and ground based observations. Recently, *Robinson et al.* [2000], hereafter to be referred to as "R2000", briefly reported the first observations using a novel experimental technique developed to artificially inject ULF waves into the magnetosphere, the effects of which could be detected by passing spacecraft. This method described by R2000 created a very localized source region for the field-guided ULF waves and resulted in the "tagging" of a very narrow flux tube, which was subsequently traversed by the FAST satellite.

[3] For clarity it seems appropriate to define the meaning of "tagging" in the context of this paper. The term is used to indicate that the ionospheric modification technique described here acts to mark a narrow flux tube by injecting along it an electromagnetic wave (i.e., an Alfvén wave) and, due to a secondary process, a characteristic electron flux. These both oscillate at the modulation frequency of the high power radio frequency radiation, which is the wave's energy source. Thus, a spacecraft with the ability to detect these fields or particles can, as in this case, identify this particular flux tube thus identifying when it is magnetically conjugate to the source region. This study demonstrates a proof of concept under conditions where the magnetic linkage between the ground and the FAST spacecraft is understood. However, the same technique may be

[1]Department of Physics and Astronomy, University of Leicester, Leicester, UK.
[2]University of California, Los Angeles, California, USA.
[3]British Antarctic Survey, Cambridge, UK.
[4]EISCAT, Ramfjordmoen, Norway.
[5]Max-Planck-Institut für Aeronomie, Katlenburg-Lindau, Germany.
[6]University of California, Berkeley, California, USA.

0148-0227/03/2002JA009483$09.00

applied when the magnetic linkage between space and ground is uncertain, for example during dynamic magnetospheric processes such as substorms and cusp transients, both very active research areas at present. Although a high power facility is required to do this artificially, the imminent deployment of the SPEAR radar [*Wright et al.*, 2000] on Spitzbergen (78 °N geographic) will open up the polar cap and cusp regions to investigation. Since most of the more dynamic regions of the magnetosphere map to these latitudes there will be an excellent opportunity to employ techniques such as this to bridge the gap between ground- and space-based observations.

[4] The EISCAT high power facility (heater) at Tromsø, Norway, has been used extensively to generate VLF, ELF and ULF electromagnetic radiations by means of modulated heating of the ionospheric conducting layers [*Stubbe et al.*, 1982, 1985; *Stubbe*, 1996]. These waves can be stimulated and launched from the ionosphere into the magnetosphere by modulating the heater output power with the desired frequencies. Modulated heating has the effect of modulating the electron temperature in the ionosphere, through the strong heating effect of the electromagnetic waves [*Stubbe and Kopka*, 1977]. Because of its dependence on electron temperature, this in turn causes the value of the electrical conductivity of the ionosphere to oscillate at the same frequencies. Thus, any preexisting natural currents, which form the ionospheric electrojet, are modulated and, as a result, the oscillating ionospheric current acts as a giant ''virtual'' antenna that transmits the VLF, ELF and ULF electromagnetic waves out into space as well as back down to the ground. Artificially stimulated waves have commonly been observed using ground-based instruments [e.g., *Stubbe and Kopka*, 1981; *Stubbe et al.*, 1981] in each of these frequency bands using VLF receivers and magnetometers (see, e.g., *Stubbe* [1996] for a review of these experiments). However, very few spacecraft observations have so far been reported and, with the exception of R2000, these were exclusively for VLF waves [e.g., *James et al.*, 1990; *Kimura et al.*, 1994]. The aim of the experiment reported by R2000 was to test the feasibility of ''tagging'' a narrow magnetic flux tube by injecting an artificially generated field-guided ULF wave and detecting the injected wave on board a spacecraft, as it traversed common field lines out in the magnetosphere.

[5] Prior to these experiments, a ray tracing study, first reported by *Wright et al.* [2000], was undertaken in order to estimate the guiding efficiency of ULF waves [e.g., *Landau and Lifshitz*, 1960] artificially excited by modulated heating. The results indicated that ULF wave frequencies of a few Hz were likely to remain field-guided, whereas VLF waves would diverge from the field line as they traveled out into space. It was determined that waves with a frequency of around 3 Hz would propagate, exhibiting Alfvénic nature, up to altitudes of 4–5 R_E and so this was the ULF wave frequency selected for the experiment. The results of ray tracing a 3-Hz wave, launched in the auroral zone, are reproduced in Figure 1 [*Wright et al.*, 2000]. The three rays depicted all have a frequency of 3 Hz but are launched with different wave normal angles, one with the k vector field-aligned and two where the k vector was nearly perpendicular to the field, one directed northward and the other equatorward. All three of the waves are strongly guided

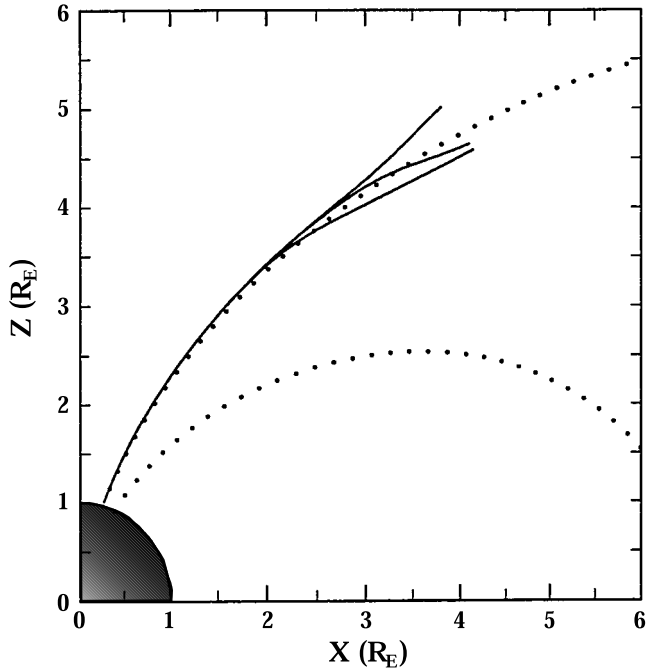

Figure 1. A raytrace of the path of a 3-Hz field-guided ULF wave injected from the ionosphere above the heater (see text for details). It is suggested that such a low frequency wave would remain field-guided to altitudes high enough for it to be detected by spacecraft, thus marking a narrow flux tube in space.

by the field regardless of the initial launch angle. The waves are launched in the left hand polarized (L-) mode, which only exists below the proton gyrofrequency in an electron-proton plasma. The R-mode also exists, and is part of the whistler mode, but this mode is not well guided along the field unless it is influenced by plasma density gradients or ducts. The rays cease to propagate at an altitude where their frequency approaches the proton gyrofrequency, where proton cyclotron damping becomes very strong. It can be seen from Figure 1 that the simulated wave achieves an altitude of 4 to 5 R_E before it is damped.

[6] The Fast Auroral Snapshot (FAST [*Carlson et al.*, 1998]) spacecraft is a low altitude orbiting satellite, which makes high time resolution measurements of the energy distribution and particle fluxes of the plasma as well as the electric and magnetic fields inside the auroral zone. The rapid sample rate of the instruments on board made FAST ideal for undertaking this experiment since it would be able to measure several cycles of a 3Hz wave as it quickly traversed the flux tube connected to the region of the heated ionosphere. An opportunity to test the feasibility of such a field line 'tagging' scheme arose on 8 October 1998, when the FAST satellite was due to pass over the site of the Tromsø heater. This site is situated just inside the Arctic Circle (69.58N, 19.22E geographic) and is within the region where the auroral electrojet commonly occurs. Experiments such as that described here generally have a relatively low success rate [e.g., *James et al.*, 1984] since a close conjunction between FAST and the Tromsø field line has to be combined with ionospheric conditions favorable to the

creation of a modest electrojet current. However, an experimental program is still ongoing in order to achieve further positive observations.

[7] One of the most significant features in the FAST satellite data shown by R2000 relates to the 3Hz modulation of the field-aligned electron flux. These authors showed that a field-parallel electric field existed above the spacecraft which accelerated the electrons. It was proposed that the observations could be explained by the nonideal MHD properties of the artificial ULF wave in the vicinity of the upper boundary of the ionospheric Alfvén resonator (IAR). It is the altitude profile of Alfvén speed, V_A, which defines the height range of the resonator. A maximum in V_A defines the upper limit of the IAR. At altitudes well below the upper boundary of the IAR the electric field of the wave is entirely perpendicular to the geomagnetic field, as seen in the spacecraft data. However, according to magneto-ionic theory [e.g., *Clemmow and Dougherty*, 1969] for waves confined to a narrow extent across the geomagnetic field, the effect of the increasing Alfvén speed as the boundary of the IAR is approached is to change the polarization of the electric field such that it acquires a component parallel to the geomagnetic field. This parallel electric field is responsible for driving a field-aligned electron flux. According to the IAR model of *Lysak* [1993], V_A is of the order of 10^3 km s^{-1} at ionospheric altitudes but increases quasi-exponentially as the plasma density of the ionized gas falls with altitude, reaching a peak of $\sim 10^5$ km s^{-1} at approximately 0.5 R_E (3200 km) above the Earth.

[8] As quoted by R2000, the ratio of the parallel, $E_\parallel$, perpendicular, $E_\perp$, components of the electric field is given by [*Clemmow and Dougherty*, 1969]

$$\frac{E_\parallel}{E_\perp} = \frac{k_\perp}{k_\parallel} \frac{\omega^2}{\Omega_i \Omega_e}, \tag{1}$$

where ω is the angular frequency of the wave, $k_\parallel$ and $k_\perp$ are, respectively, the components of the wave vector, parallel and perpendicular to the geomagnetic field and Ω_i and Ω_e are the ion and electron gyrofrequencies, respectively. It is assumed that the heated patch has a Gaussian shape of width L, across the geomagnetic field and, therefore, the characteristic width of the spatial spectrum normal to the geomagnetic field will be $1/L$. Further, the value of $k_\parallel$ is ω/V_A, providing $L \gg V_A/(\Omega_i\Omega_e)^{1/2}$, which is well satisfied for the heated patch under consideration. Hence, equation (1) can be written

$$\frac{E_\parallel}{E_\perp} = \frac{V_A \omega}{L \Omega_i \Omega_e}. \tag{2}$$

[9] Equation (2) indicates that $E_\parallel$ becomes significant close to the peak of the Alfvén speed profile, at the upper boundary of the IAR. Using the model values of V_A from *Lysak* [1993] it can be shown that $E_\parallel/E_\perp$ increases by three orders of magnitude in moving from the ionosphere to this boundary. This model also implies that the region of highest $E_\parallel$, the source region of the modulated electron flux, is somewhere in the altitude range 3250–3550 km.

[10] As stated by *Robinson et al.* [2000], in order to account for the existence of a parallel electric field in the vicinity of the upper boundary of the Ionospheric Alfvén Resonator (IAR) it is necessary to deviate from ideal MHD and consider the effects of electron inertia. In this case the Alfvén dispersion relation becomes

$$\omega = \frac{k_\parallel \cdot V_A}{\sqrt{1 + \frac{k_\perp^2 c^2}{\omega_p^2}}}, \tag{3}$$

where ω_p is the plasma angular frequency and c is the speed of light. Wave propagation remains Alfvénic while

$$\sqrt{1 + \frac{k_\perp^2 c^2}{\omega_p^2}} \approx 1 \tag{4}$$

i.e., while $k_\perp \ll \omega_p/c$ or $\lambda_\perp \gg 2\pi c/\omega_p$. In the ionosphere $2\pi c/\omega_p$ is $\sim$100 m and at 3000 km altitude is $\sim$30 km. The change in $\lambda_\perp$ over this height range is due to dipole field geometry. Thus, the field line tagging process remains effective up to about 3000 km and the waves are contained within the flux tube bounded by the source region.

[11] Whereas R2000 presented measurements made by FAST and attempted to explain the observations in the context of the artificial ULF waves interacting with the upper boundary of the IAR, this paper presents data pertaining to the ionospheric conditions which occurred during that experiment and discusses their significance with regards to the mechanism leading to the FAST observations. The role of substorm activity in defining the nature of the artificial ULF waves is also investigated.

2. Instrumentation

2.1. FAST Spacecraft

[12] The FAST spacecraft was launched on 21 August 1996 into an elliptical orbit with a perigee and apogee of 350 km and 4175 km, respectively, and an inclination of 83° [*Carlson et al.*, 1998]. It was primarily designed to make high spatial and temporal resolution measurements of the plasma and electric and magnetic fields in the low altitude auroral acceleration region.

2.1.1. Electrostatic Analyzers (ESAs)

[13] In total there are 16 electrostatic analyzers (ESAs), each of which measures the ion and electron pitch angle distributions over a 180° field of view. The particles are imaged, according to their energy per unit charge, onto a microchannel plate detector. Pairs of the analyzers, on opposite sides of the spacecraft, are grouped to provide an overall field of view of 360°. There are four ESA stacks located at 90° intervals around the spacecraft. Three Stepped ESA (SESA) analyzers, which are operated as spectrometers to obtain high time resolution (1.7 ms) electron measurements in 16 pitch angle bins, are included in each of these stacks. The remaining analyzer in each stack is configured as either an ion or electron spectrometer (IESA or EESA), used to make high resolution distribution measurements with 32 pitch angle bins every 70 ms [*Carlson et al.*, 1998]. When the spacecraft is in the auroral zone, the analyzer's field of view lies in the spacecraft spin plane and is typically aligned within $\sim$6° of the magnetic field. The measurable energy range is 4 eV to 30 keV for electrons and 3 eV to 25 keV for ions. The electron flux measurements

presented in this paper (and R2000) were recorded exclusively by the SESA instruments.

2.1.2. Electric Field Sensors

[14] The FAST electric field instrument consists of ten spherical sensors, two each on four 28 m long radial wire booms and one on each of two axial stacers. The spheres on each wire boom are located at 23 m and 28 m from the spacecraft. The axial spheres are separated from each other by 8 m. Despite the fact that one of the wire booms failed to deploy properly, the remaining three booms are adequate to measure vector electric fields. Each sphere houses a preamplifier circuit and the electric field is derived from the voltage difference between two spheres. The spheres can also be operated in a Langmuir probe mode to measure plasma density. DC level signals and those with frequencies up to about 2 MHz are processed by the instrument, which has a dynamic range of 100 dB. Measurements produced by the sensors include continuous waveform capture at 2000 samples s^{-1}, burst waveforms up to 2×10^6 samples s^{-1}, and electric field spectra between 16 Hz and 2 MHz.

2.1.3. Magnetic Field Sensors

[15] The magnetic field instruments on board FAST include both a DC fluxgate magnetometer and an AC search-coil magnetometer. The former is a three-axis instrument using low noise ring core sensors that are mounted on a boom extending 2 m from the spacecraft. The search-coil magnetometer uses a three-axis sensor system that provides AC magnetic field data over the frequency range 10 Hz to 2.5 kHz on two axes while the third axis response extends to 500 kHz. The fluxgate magnetometer is designed to measure fields of up to ±60,000 nT. With digitization to 16 bits, the sensor has a resolution of ±1 nT, although fields can be measured to higher accuracy through averaging.

2.2. EISCAT UHF Radar System

[16] The European Incoherent Scatter (EISCAT) UHF radar [e.g., *Rishbeth and Williams*, 1985; *Rishbeth and van Eyken*, 1993] is often operated in support of artificial modification experiments by the Tromsø heater (see section 2.3). The SP-UK-HEAT experiment on 8 October 1998, included UHF radar operation, with the transmit/receive antenna at Ramfjordmoen near Tromsø, Norway, aligned approximately along the local magnetic field direction (geographic azimuth: 183.2°, elevation: 77.2°) The remote site UHF receivers at Kiruna, Sweden (67.9°N 20.4°E geographic), and Sodankylä, Finland (67.4° N 26.6°E geographic), intersected the transmitter beam at the *F* region altitude of 250 km. Four pulse schemes were transmitted; long pulse, alternating code and two power profiles. The long pulse scheme provides observations of electron density, ion and electron temperature and line-of-sight ion velocity over 21 range gates along the Tromsø beam, from approximately 140 to 600 km altitude with a gate separation of ~22 km in altitude. High altitude resolution observations (~3.1 km) of these parameters in the *E* and lower *F* regions are obtained from the alternating code pulse scheme. The two short power profile pulses yield estimates of raw electron density at ~3.1 km and ~4.4 km altitude resolution through the *D*, *E*, and lower *F* regions; the former provides the zero lag lacking in the alternating code autocorrelation function. The tristatic nature of the EISCAT UHF radar enables the three-dimensional ion velocity to be determined in the intersection volume of the three receiver beams.

2.3. EISCAT High Power RF Heater

[17] Collocated with the EISCAT UHF radar (see section 2.2) at Tromsø is the EISCAT "heater", which is a high power radio frequency facility [see *Rietveld et al.*, 1993]. It consists of 12 transmitters feeding one of three 6 by 6 arrays of crossed dipole antennas, which can be phased to transmit O-, X- or linear mode signals and cover a total frequency range of 3.9–8.0 MHz. During the experiment on 8 October 1998, array 2 was employed, which has a frequency range of 3.9–5.6 MHz. The Heater is capable of radiating over 1 MW of continuous wave power, which may be modulated. During this experiment, an X-mode signal was radiated by the heater at a frequency of 4.04 MHz, with an imposed dual modulation of 3 Hz and 1 kHz. The total output power of the heater was 960 kW, which corresponds to an effective radiated power of 144 MW, assuming an antenna gain of 21.8 dBi on array 2 as predicted by the antenna modeling program NEC2. The heater beam, which has a full width of 14°, at the 3dB level, was centered on the field-aligned direction and produced a roughly circular heated layer in the *E* region ionosphere of diameter 25 km, approximately 100 km above the ground, which acted as the source region of the artificial ULF waves. The thickness of the active source region of the ULF waves is defined by the electron density scale height in the region of interaction. In the lower D-region this is of the order of 5 km.

2.4. Ground Magnetometers

[18] Magnetic fluctuations associated with the background magnetic field as well as those associated with the artificial ULF waves were recorded by ground magnetometers. Large scale changes in the ambient field were detected using in the IMAGE (International Monitor for Auroral Geomagnetic Effects) chain of magnetometers located in northern Scandinavia [e.g., *Lühr*, 1994]. The stations used range in geomagnetic latitude from 63.25°N at Pello (PEL) to 71.25°N at Bjørnøya (BJN). The magnetometer data have a time resolution of 10 s and are reproduced in an XYZ (geographic) coordinate system. In addition, a high temporal resolution "pulsation magnetometer", with a sampling frequency of 10 Hz, located at Kilpisjärvi, Finland (65.78° N 104.31°E geomagnetic) was employed to measure the ground magnetic signature of the artificial ULF waves. The data from this instrument are presented in HDZ (geomagnetic) coordinates. The spatial resolution of ground magnetometers is determined by the way in which they integrate information over an area with a scale length of the order of the *E* region height (~120 km), as discussed by *Hughes and Southwood* [1976].

3. Observations

[19] A run of the SP-UK-HEAT experiment occurred on 8 October 1998 from 2015 to 2043 UT. The FAST spacecraft passed through the magnetic field lines which threaded the region of the ionosphere illuminated by the heater. As described in section 2.3 a dual modulation of 3 Hz and 1 KHz was imposed on the heater signal. The VLF frequency was also included so that the resultant nonguided (i.e.,

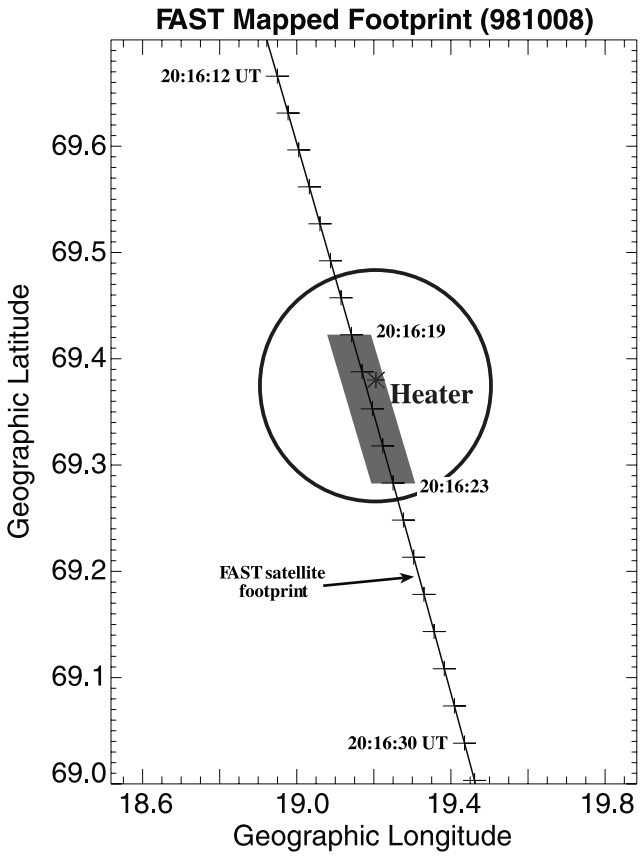

Figure 2. The ionospheric footprint, mapped along the geomagnetic field to an altitude of 100 km, of the disturbance seen in the satellite data, for 4 s, between 2016:19 and 2016:23 UT (shaded portion of the footprint). Also included is the heated patch of the *E* region ionosphere, the circle indicating the 3 dB power level of the heater beam.

divergent or isotropic) waves could be detected outside the region of the narrow flux tube containing the ULF waves. However, this paper will discuss only the ULF waves generated by the 3-Hz modulation and not those waves resulting from the VLF modulation. Figure 2 depicts the ionospheric source region (indicated by the 25 km diameter circle) together with the ionospheric footprint of the FAST satellite track, mapped down the field line into the *E* region. The IGRF model appropriate for 8 October 1998 was used for this mapping. The satellite altitude during this transit was approximately 2550 km. The shaded part of the FAST footprint in Figure 2 indicates the interval over which the spacecraft detected the artificial ULF waves. It should be noted that this figure supersedes Figure 1 of R2000. Due to an oversight, Figure 1 of R2000 fails to account for the 12° southward tilt of the heater beam during field aligned operation. Thus, the interval over which FAST detected the artificial ULF waves translates to a spatial region which is coincident with the heated *E* region, indicating that these waves remained field-guided at least up to the altitude of FAST. However, as a result of higher altitude current systems, the IGRF is probably only applicable below about 1 R_E and field line mapping using this model becomes increasingly difficult at higher altitudes, which illustrates the importance of field line tagging.

[20] Ionospheric conditions over Tromsø and inside the region disturbed by the heater are indicated in Figure 3, which illustrates the EISCAT UHF observations in the altitude range 70–500 km for the interval 1900 to 2100 UT. Panels 3a, c, d and e of the figure present long pulse estimates of *F* region electron density, electron temperature, ion temperature and line-of-sight ion velocity, respectively, as a function of altitude, from 150 to 500 km, along the Tromsø beam. Positive (blue) line-of-sight velocities indicate motion toward the radar, corresponding to flow down the field line. Figure 3b depicts raw electron density estimates from the low altitude, high resolution (∼4.4 km) power profile scheme, to a maximum altitude of 150 km in order to match the lower altitude of the long pulse observations presented. Figure 3f illustrates the field-perpendicular eastward and northward components of the ion velocity derived at the *F* region tristatic altitude of 250 km. Figure 3g presents estimates of the height-integrated Pedersen (red trace) and Hall (blue trace) conductivities—also referred to as the Pedersen and Hall conductances [e.g., *Brekke and Moen*, 1993]—based on the raw electron densities from the low resolution power profile [e.g., *Lester et al.*, 1996]. The long pulse and power profile (and hence height-integrated conductivity) observations are at a temporal resolution of 10 s; the field-orthogonal velocity components are at 30 s resolution. The vertical dashed line indicates the time at which the FAST satellite traversed the heated patch.

[21] X-component data from several of the IMAGE ground magnetometers are reproduced in Figure 4a [after R2000] is one of the field-perpendicular components of electric field measured at the spacecraft. This component was aligned with the direction of travel of the satellite. Unfortunately, since there are no data from the electric field sensors mounted on the axial stacers, a second field-perpendicular component of the electric field is unavailable. The 3-Hz wave visible against a slowly varying background from 2016:19 to 2016:23 UT in Figure 5a, exhibits a maximum amplitude of approximately 10 mV m^{-1}. Figures 5b and 5c respectively show the downward and upward field-aligned fluxes of electrons with energies 37, 74 and 149 eV, measured by the SESA within 30° of field-aligned. Although the structure of the 3-Hz wave signature is more complex in the downward electron flux (Figure 5b), the 3-Hz wave signature is most clearly observed in all three energy channels in the interval 2016:20–2016:22 UT, although another less distinct enhancement in the downward electron flux associated with the wave is also apparent from 2016:19 to 2016:20 UT. The wave is energy dispersed, being observed in the highest energy channel first. There is little or no sign of any wave signature in the upgoing electrons plotted in Figure 5c. Power spectra of the 37 eV downgoing electron flux and perpendicular electric field are reproduced in Figures 6a and 6b respectively. Each panel of Figure 6 shows 3 consecutive 4 s spectra in the interval 2016:15–2016:27 UT, arranged to that the second spectrum covering the interval 2016:19–2016:23 UT encapsulates the 3-Hz signature in both the electric field and downgoing electron flux data. A clear spectral peak is evident in both cases at this time but is absent or weak in the 4 s intervals immediately prior to and following this.

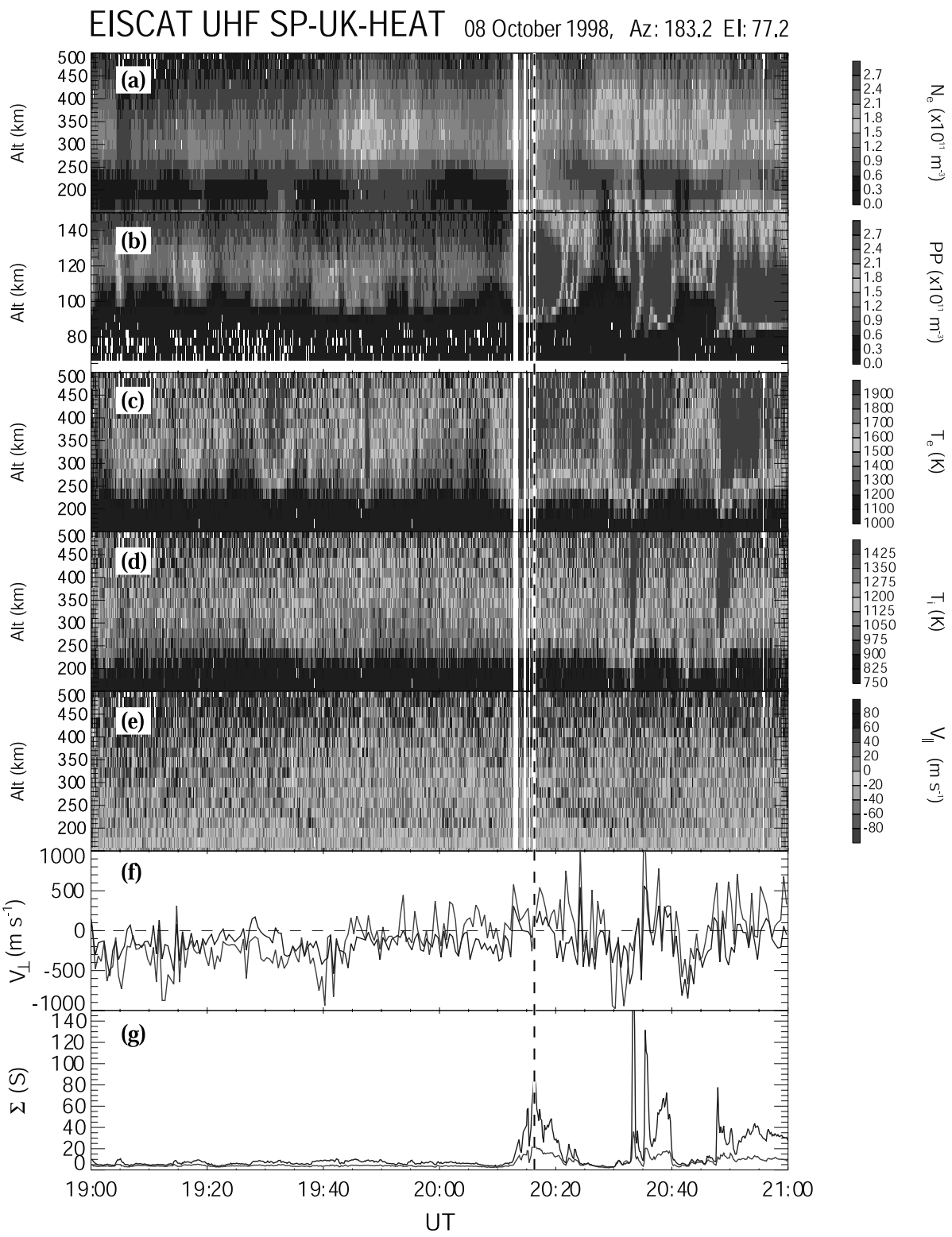

Figure 3. Data parameters measured by the EISCAT UHF radar during the run of SP-UK-HEAT on 8 October 1998. Plotted as a function of altitude along the field-aligned Tromsø beam (geographic azimuth: 183.2°, elevation: 77.2°) are: (a) *F* region electron density, (b) *D* and *E* region electron density derived from power profile, (c) *F* region electron temperature, (d) *F* region ion temperature and (e) *F* region line-of-sight ion velocity. Panel f illustrates the field-perpendicular eastward (red) and northward (blue) components of the ion velocity derived at the *F* region tristatic altitude of 250 km. Panel g, presents height-integrated Pedersen (red) and Hall (blue) conductivities. The dashed vertical line indicates the time at which FAST traversed the field line along which the UHF radar was observing. See color version of this figure at back of this issue.

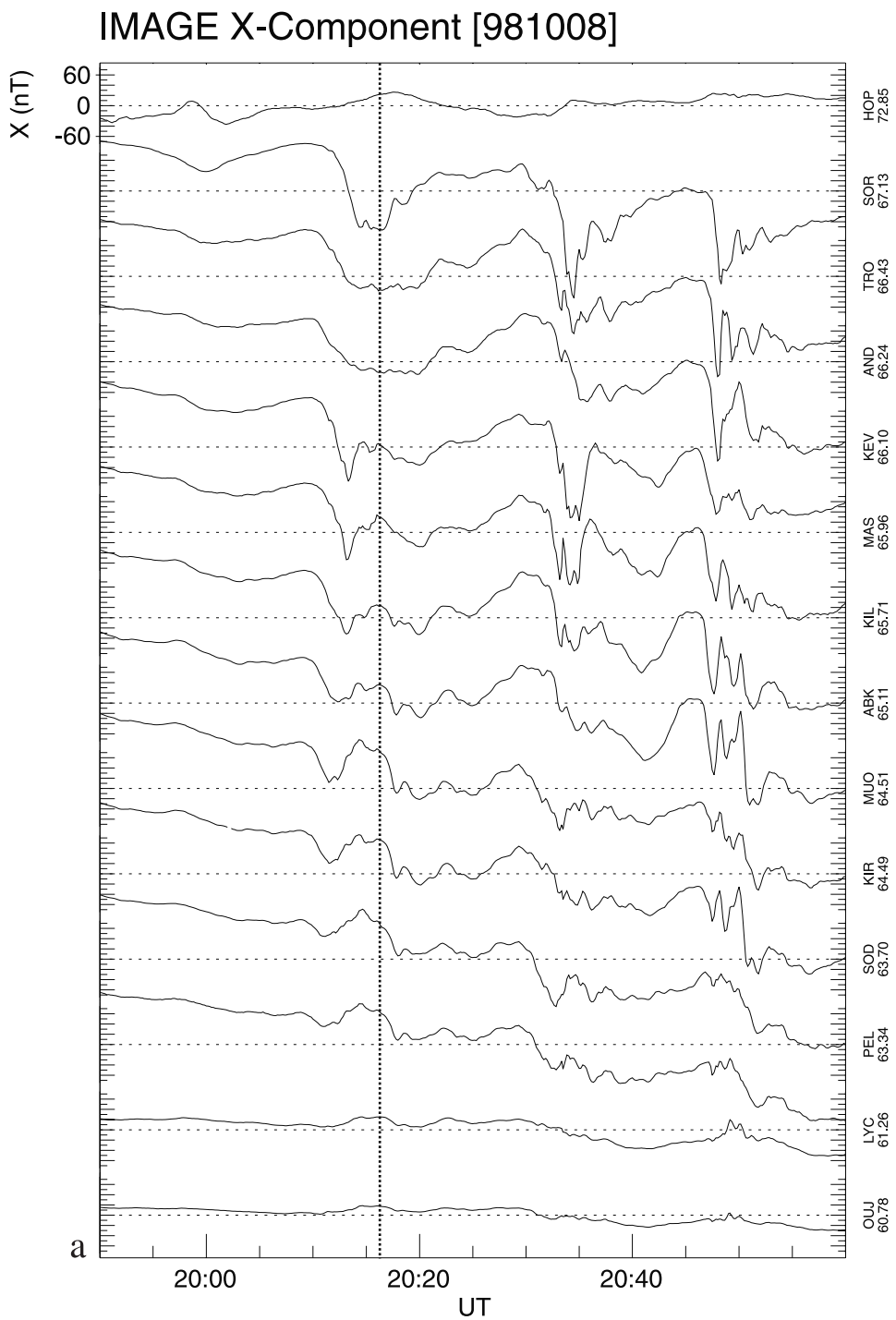

Figure 4. (opposite) a: X-component data from the IMAGE magnetometer array in Scandinavia for the interval 1950–2100 UT on 8 October 1998. Stations are arranged in order of increasing geomagnetic latitude. The vertical dotted line indicates the time at which FAST traversed the region conjugate to Tromsø (TRO). b: The same data illustrated in (a) filtered to exclude periods outside the range 20–200 s in order to indicate Pi2 signatures. The vertical dashed lines mark the approximate start of distinct Pi2s, each associated with a substorm expansion phase onset.

This demonstrates the localization of the 3-Hz signal in the FAST data.

[23] In order to determine more clearly the interval over which the artificial ULF waves were detected by FAST, a dynamic spectral analysis was performed on the data (see Figure 7). Panels a–c of Figure 7 represent respectively the temporal variation of the 3-Hz spectral component in the downward electron flux, the perpendicular electric field and the "outward" component of the magnetic field for the interval 2016:15–2016:27 UT. In this coordinate

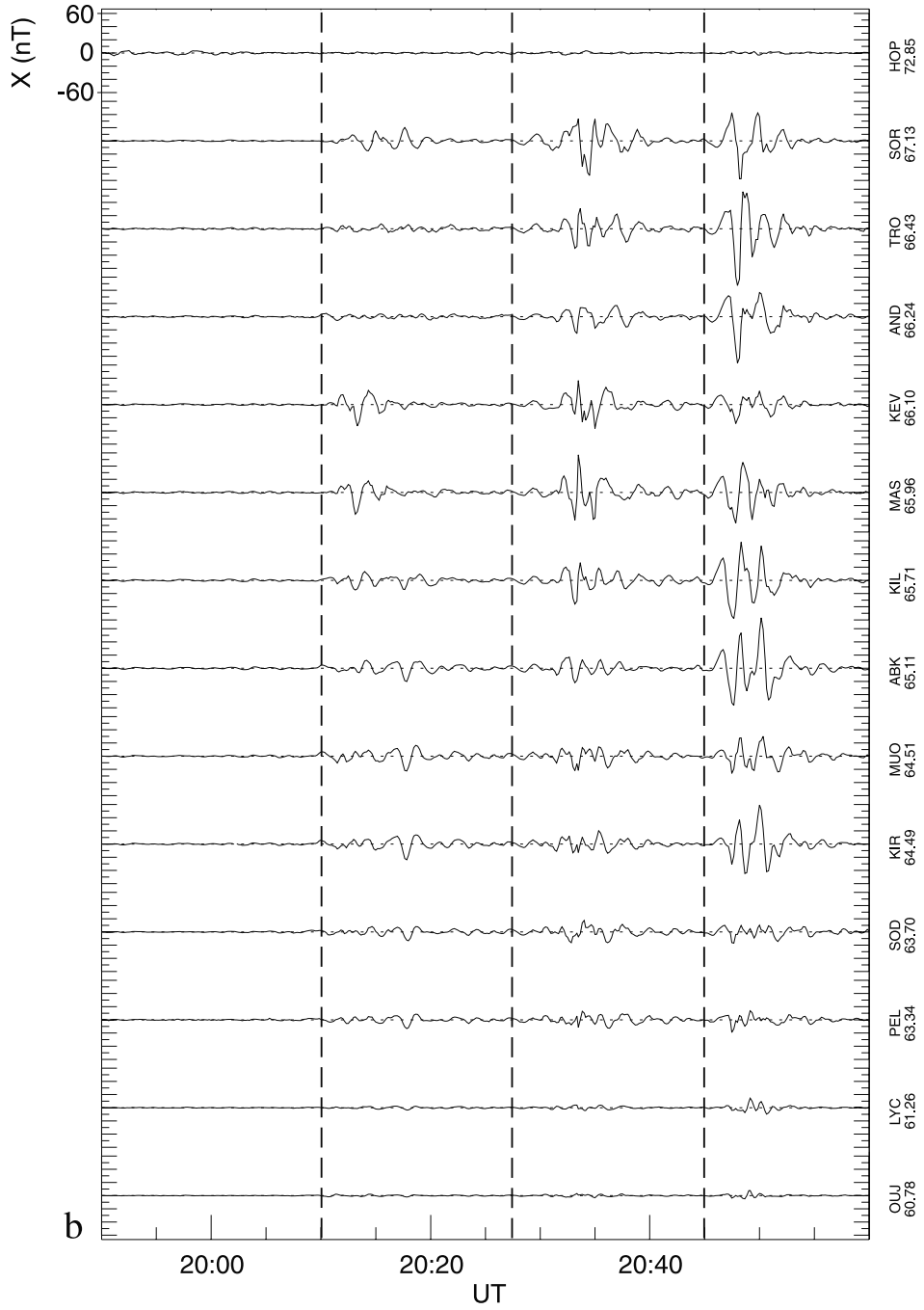

Figure 4. (continued)

system, outward forms the right-handed set with the field-aligned and eastward components and is, therefore, essentially directed northward for the data presented here. At times a spacecraft generated signal at 4 Hz (0.25 s period) is measured by the magnetometer. The source of this anomalous signal has not been determined. Unfortunately this spurious signal is very close in frequency to 3 Hz, and masks the 3-Hz magnetic signal in the time series, which are therefore not shown here. In each case a 2 s sliding spectral window, with a 0.1 s slip was employed. A minimum of 2 s was required in order to be able to resolve the 3-Hz signature from the 4-Hz contamination in the magnetic field data. The power in the 3-Hz spectral component derived from downward electron flux (Figure 7a) displays two enhancements. The first occurs from 2016:16.5 to 2016:18.5 UT (Interval 1) when there is no equivalent enhancement in the 3-Hz component of electric and magnetic fields. The second increase, which occurs in the interval 2016:19.5–2016:23 UT (Interval 2), appears simultaneously with those in the electric and magnetic field data (Figures 7b and 7c respectively). It is worth noting that when a shorter spectral window is applied to the downward electron flux data, Interval 2 in Figure 7a is resolved into two distinct bursts which correspond, respec-

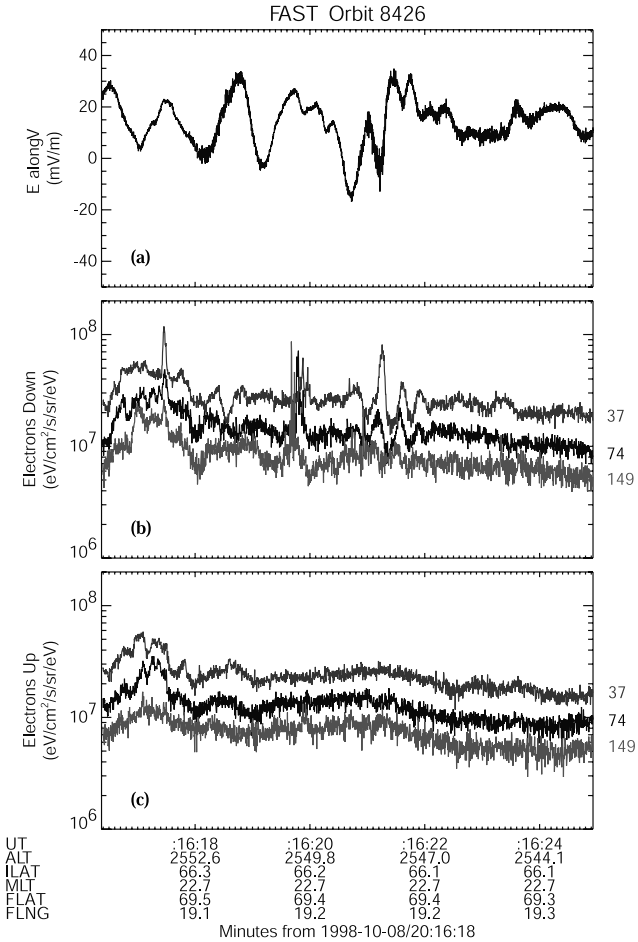

Figure 5. The data measured by the FAST spacecraft from 2016:16 to 2016:25 UT on 8 October 1998 (orbit 8426): (a) the field-perpendicular electric field, measured along the direction of the spacecrafts flight path; (b) the downgoing and (c) the upgoing electron flux for the 37, 74 and 149 eV energy channels.

tively, with the increase in downward electron flux (see Figure 5b and also R2000) occurring from 2016:19.5 to 2016:20 UT and the clear wave packet observed in the same flux shortly afterward at 2016:20.5–2016:22 UT. Interval 2, identified in Figure 7, occurs when the wave signature in the downgoing electron flux (Figure 5b) exhibits energy dispersion. In contrast, the enhancement in the 3-Hz spectral power of this flux observed Interval 1 is dispersionless and also does not appear in the electric and magnetic field components (Figures 7b and 7c). The significance of this dispersion will be discussed in section 4. To complement the observations of the artificial ULF wave in the downward electron flux during Interval 2, there is an enhancement of the 3-Hz spectral power in the perpendicular electric field (Figure 7b). A weak enhancement of the 3-Hz spectral power was also detected in the outward (northward) component of the magnetic field measured at the spacecraft (Figure 7c).

[24] In addition to its detection in the magnetosphere, the pulsation magnetometer located at the ground in Kilpisjärvi, Finland also detected the magnetic signature of the artificial waves. The heater generates coupled Alfvén and fast mode waves in the ionosphere which propagate out into the magnetosphere. Clearly, the Alfvén waves are field guided and are thus important from the point of view of the spacecraft measurements and the tagging of the field line. Below the ionosphere, wave energy propagates as a free space electromagnetic wave and it is this which is detected by the ground magnetometer. As a result of ionospheric screening effects [see *Hughes and Southwood*, 1976] the amplitude of such signals fall off as $e^{-k_{\perp}z}$, where at the ground z is the E region height. The ground signal will thus be very weak. Power spectra of the H-, D- and Z-component magnetometer data are illustrated in Figure 8a, in which a clear peak is observed at a frequency of 3 Hz. These spectra indicate a weak signal at the ground. However, it is to be expected that the signature will be weak since the magnetometer was located approximately 90 km south-east of the EISCAT facility at Tromsø and well outside the ground projection of the heated region of the ionosphere. Nevertheless, the artificial wave amplitude was measurable at the ground. The upper panel of Figure 8b indicates the

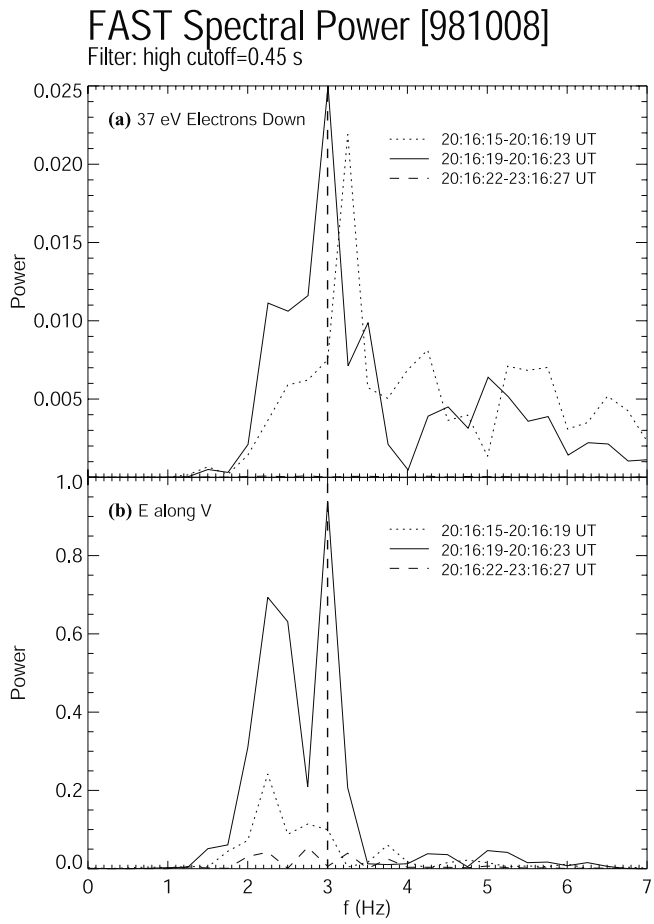

Figure 6. Power spectra for (a) the downgoing 37 eV electron flux and (b) the perpendicular electric field measured at FAST. Both panels display consecutive spectra using a 4 s spectral window in the interval 2016:15–2016:27 UT. A long period cut-off of 0.45 s was applied in each case. The vertical dashed line represents the position of the 3-Hz spectral component.

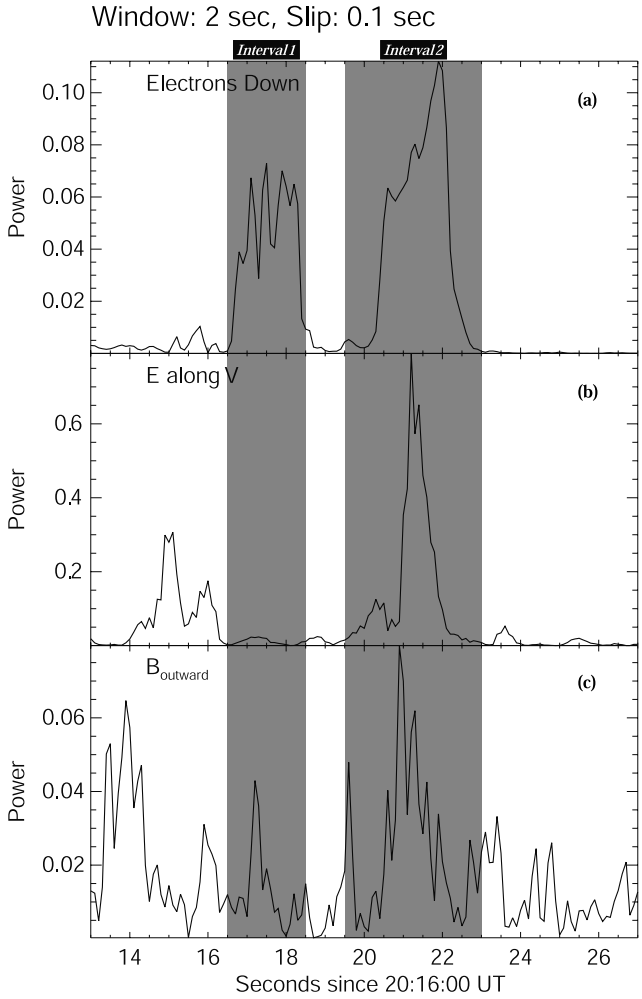

Figure 7. The temporal variation of power of the 3-Hz spectral component derived from a dynamic spectral analysis of (a) the downgoing flux of 37 eV electrons, (b) the perpendicular electric field (along the spacecraft trajectory) and (c) the outward component of the magnetic field measured by the FAST spacecraft for the data interval shown in Figure 5. In each case a 2 s spectral window and a slip of 0.1 s was employed.

time variation of the 3-Hz spectral power for the interval surrounding the experiment. It can be seen that the greatest enhancements of the 3-Hz magnetic signature detected on the ground occurred while the heater output was being modulated. There is some indication that there may be a correlation between the temporal variations of the 3-Hz spectral power and the changes in the height integrated conductivities measured by EISCAT, which are displayed in the lower panel of Figure 8b (reproduced from Figure 3g). There are no magnetometer data available prior to 1946 UT and no EISCAT conductivity measurements after 2100 UT.

4. Discussion

[25] R2000 presented data which indicated that an artificial ULF wave, generated by a high power modification technique, was detected by the FAST spacecraft as it traversed the field lines which mapped to the heated region. The flux tube which carried the ULF wave energy was narrow, being defined by the circular heated patch of ~25 km diameter. This diameter remains relatively small when mapped out to the altitude of the spacecraft (~2550 km). *Stubbe and Kopka* [1977] modeled the flows excited inside the heated volume. They demonstrated that although eddy currents would be excited around the heated region, these would still be confined to an area not much larger that the heated region itself [see *Stubbe and Kopka*, 1977, Figure 2]. In fact the magnitude of the currents excited outside the region directly affected by the heater fall off as $1/r^2$, where r is the distance from the center of the heated patch. Thus, the artificial waves are confined to the narrow flux tube bounded by the edge of the heated E region.

[26] Although the experiment generated both isotropic (known as the fast mode) and field-guided waves (transverse Alfvén waves), only the latter type were significant to the spacecraft measurements, since those observed by FAST were localized to the Tromsø flux tube, which is consistent with the waves being field-guided. The spatial extent of the flux tube is defined by the 4 s interval over which the 3-Hz waves were detected. Since the wave observed by FAST was Alfvénic, the electric and magnetic signatures associated with the wave should be mutually orthogonal and perpendicular to the geomagnetic field. As noted previously, only one field-perpendicular component of the electric field was measured by FAST (due to a lack of data from one set of sensors) and so it is not possible to demonstrate unequivocally that it is orthogonal to the weak magnetic signature, which occurs in the "outward" direction of a field-aligned coordinate system. However, the measured electric field could represent a component of that which should, if the wave is truly Alfvénic in nature, be directed eastward in this coordinate frame.

[27] It can be seen from Figure 2 that the footprint of the FAST spacecraft, mapped to an altitude of 100 km, during the interval when the 3-Hz signature was detected by the electric and magnetic field sensors on the spacecraft (indicated by the shaded area on the footprint track in Figure 2), corresponds very well to the area of the E region illuminated by the Heater. This implies that the artificial ULF waves were still confined inside a narrow flux tube at the altitude of the spacecraft (2550 km). The substorm activity and associated electron precipitation shortly before the FAST conjunction caused a reduction of ~100 nT in the X-component (north-south) of the magnetic field measured on the ground at 2010 UT. In order to assess the significance of the field deviation from the IGRF under these conditions a simple model of the magnetic field associated with the enhanced electrojet current was employed. The model simulated the latitudinal spatial extent of the electrojet as a series of distributed infinitely long and narrow line currents at the E region height and the magnetic field associated with this structure was calculated using the Biot-Savart law. Currents induced in the Earth's crust by the E region current system were also simulated using the complex image method of *Boteler and Pirjola* [1998]. The current in the system was scaled until it provided the 100 nT reduction in the ambient field observed at the ground. This technique indicated that the electrojet current in this case

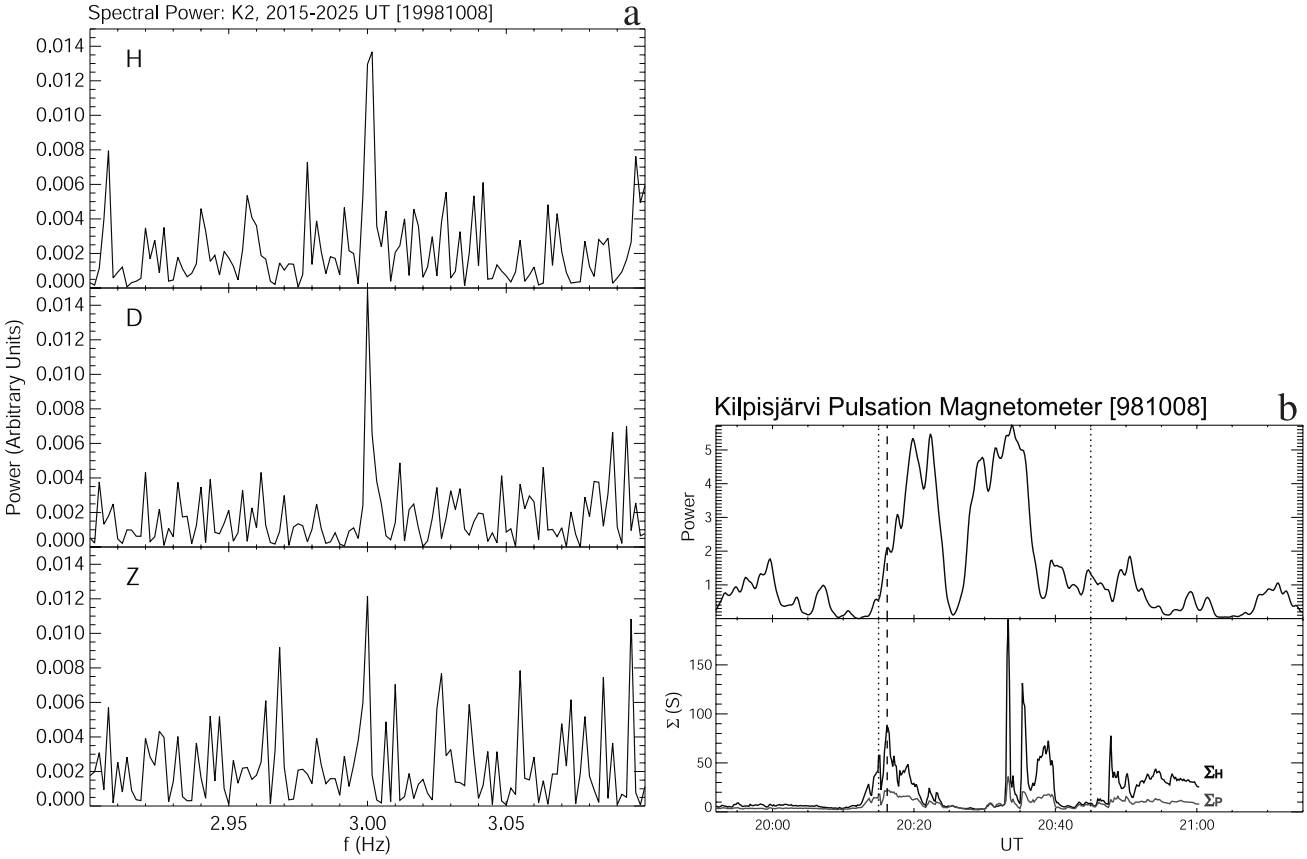

Figure 8. a: Power spectra for the interval 2015–2025 UT derived from the H-, D- and Z-component data recorded by the Kilpisjärvi pulsation magnetometer. b: The temporal evolution of the 3-Hz spectral component (upper panel) derived from the dynamic spectrum of the H-component data recorded by the Kilpisjärvi pulsation magnetometer. A 10 min sliding window with a 10 s slip was employed in the analysis. Also reproduced (lower panel), from Figure 3g, are the height integrated ionospheric Hall and Pedersen conductivities (Σ_H and Σ_P respectively). The vertical dotted lines enclose the interval when the Tromsø heater was transmitting its modulated signal and the vertical dashed line indicates when the FAST spacecraft was conjugate to Tromsø.

would only cause the IGRF mapping of FAST to the *E* region altitude to deviate by 1–2 km. Thus, this change is considered insignificant for this study.

[28] R2000 suggested that, due to the factor of $k_\perp$ in equation (1), perpendicular to the geomagnetic field the spatial distribution of $E_\parallel$ at the upper boundary of the IAR will be a derivative of the Gaussian spatial distribution of $E_\perp$. As a result $E_\parallel$ will be oriented upward in one half of the disturbed region and downward in the other. R2000 therefore proposed that the spacecraft would only detect accelerated electrons (traveling downward) in one half of the disturbed region. In the other half of this region, $E_\parallel$ will be oriented downward and will thus accelerate electrons upwards from the upper boundary of the IAR and away from the spacecraft. This situation is illustrated schematically in Figure 9. Due to the 3-Hz oscillation of the electric field, the situation reverses every half cycle and thus electrons are accelerated away from the boundary first upwards then downward causing the measured electron flux to also vary at 3 Hz. The largest amplitude of $E_\parallel$ occurs where the spatial gradient of $E_\perp$ maximizes. In fact, in the center of the active region, where there is a node of $E_\parallel$, the measured electron flux would be expected to fall to zero [see R2000; *Kolesnikova et al.*, 2002]. This hypothesis is certainly consistent with the observations (see Figure 5b), where the two energy dispersed signatures in the downgoing electron flux from 2016:19.5 to 2016:20 UT and from 2016:20.5 to 2016:22 UT represent the locations of maximum $E_\parallel$ (roughly corresponding to the two "edges" of the gaussian profile of $E_\perp$ across the active flux tube traversed by FAST see Figure 9). It is possible that the difference in the physical form of the downward electron flux at these two times is related to spatial asymmetries in the electric field profile generated by the heater.

[29] Since the downward traveling electrons observed in Interval 2 are energy dispersed (Figure 5b), it has been possible to undertake a time-of-flight analysis of the spacecraft data in order to identify the source altitude of this field-aligned flux [*Cash et al.*, 2002]. Clearly the source region is above the spacecraft since only the downgoing 3-Hz electron flux is observed. *Cash et al.* [2002] assumed that the parallel electric potential varied exponentially with altitude, maximizing at the upper boundary of the IAR, and with time through the Alfvén wave

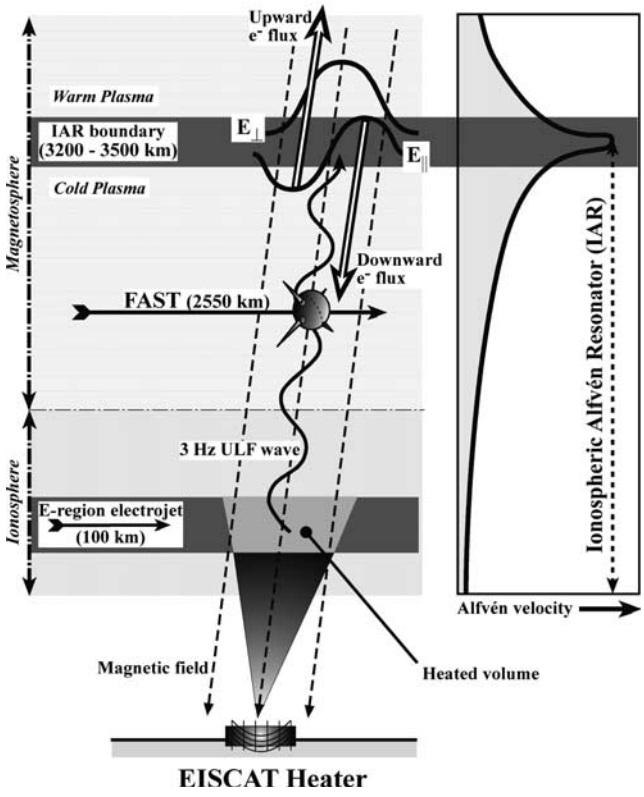

Figure 9. A schematic of the artificial 3-Hz ULF wave injection from the ionospheric source region, along the geomagnetic field line, beyond the spacecraft to the Ionospheric Alfvén Resonator boundary at about 1.5 R_E. Here the wave acquires a significant electric field component parallel to the geomagnetic field and can accelerate electrons down past the spacecraft toward the ionosphere, as well as away from the spacecraft, out into space.

cycle. The variation of the parallel electric potential in the frame of reference of an electron was calculated by extrapolating upwards from the spacecraft; each electron channel was considered separately. The parallel electric potential experienced by an electron of a given energy at each increment in altitude was found by iteration, and from this the electric field and electron velocity and flight times were calculated as a function of altitude. The upper boundary of the IAR is indicated by the minima in the electron velocity profile. The altitude of the upper boundary of the IAR and, thus, the altitude of the maximum amplitude of the parallel electric field component, calculated by this method was found to be 3400 ± 100 km (i.e., 850 ± 100 km above the spacecraft), which is in agreement with previous, less complete models. A more detailed description of this model is given by *Cash et al.* [2002]. In contrast to the 3-Hz wave activity observed in Interval 2, it should be noted that the enhancement of the 3-Hz spectral power in the downward electron flux measurements from Interval 1 (Figures 5b and 7a) occurs simultaneously in the upward and electron flux and that the associated 3-Hz signatures in the electron fluxes are not, in this case, energy dispersed. Thus, the source of this wave energy is not the same as that for Interval 2. It is reasonable to conclude therefore that electron fluxes observed in Interval 1 are the result of some naturally occurring process rather than being related to the heating experiment.

[30] Recently, *Kolesnikova et al.* [2002] estimated the effect, in the inner magnetosphere, of modulated X-mode heating of the lower ionosphere, incorporating the EISCAT UHF radar observations during the FAST overpass. The authors followed the work of *Borisov and Stubbe* [1997], who constructed a quantitative model of the generation of three-dimensional polarization currents due to periodic heating, which produce magnetic disturbances on the ground and Alfvén waves propagating upward from the heating layer. *Kolesnikova et al.* [2002] developed this model for the conditions of strong electron precipitation appropriate to this particular experiment. The majority of the heating effect was found to occur between 80 km and the heater reflection height of 87 km. The authors remark that during such strong precipitation, the primary current caused by the perturbation in the conductivity in the heated region is closed entirely by a field-parallel current and it is, in fact, under such circumstances that conditions at the magnetosphere-ionosphere boundary are the most favorable for launching Alfvén waves. The quantitative estimates from the model of *Kolesnikova et al.* [2002] gave a value of the transverse electric field consistent with that observed by FAST and revealed a parallel electric field of the order 10 μV m^{-1} which, the authors speculated, could be effective in accelerating superthermal electrons downward into the ionosphere. The model, however, underestimates the expected amplitude of the perpendicular electric field measured at the spacecraft by an order of magnitude. Taking this into account, it can be inferred from the model that the expected amplitude of the magnetic signature of the wave at the spacecraft should be of the order of 0.1 nT, which is considerably smaller than is indicated by the observations presented in this study.

[31] *Kolesnikova et al.* [2002] speculated that the substorm was important in the success of the experiment. This point is considered in more detail here. Ultimately, it is the artificial modification of the local ionospheric Pedersen conductivity, σ_p, by the Tromsø heater that was responsible for launching the Alfvén wave during this experiment. σ_p is proportional to the product of the local electron density, N_e, and the local electron-neutral collision frequency, ν_{en}. Thus, if heater radio wave angular frequency, $\omega \gg \nu_{en}$ then the heater-induced change in the conductivity, $\Delta\sigma_p$, will be related to $N_e\Delta\nu_{en}$, where $\Delta\nu_{en}$ is the perturbation caused by the action of the heater. Changes in electron density occur on timescales considerably longer than the 3-Hz modulation. The most significant effect of the substorm, which commenced at 2010 UT on 8 October 1998, was the large enhancement of electron density, N_e, inside the *D* and *E* region ionospheres. The energetic particle precipitation resulted in at least a ten-fold increase in plasma density compared to the presubstorm level, as evident in Figures 3a–3b. As a result the heater pump wave (at 4.04 MHz) was reflected at an altitude of ~87 km leading to significant deviative absorption of the HF wave in the *D* region. *Kolesnikova et al.* [2002] demonstrated that 90% of the pump energy was absorbed in the *D* region in the altitude range 80–87 km. Their model suggests that the $\Delta\nu_{en}$ caused by the action of the heater, in this case, would have

lead to a $\Delta\sigma_p/\sigma_p$ of $\sim$2–3. This would not have been achieved had the pump wave reflected at a higher altitude since ν_{en} is greatest in the *D* region. Although artificial modification of the *D* and *E* region ionosphere is always likely to generate such ULF waves in this way [e.g., *Borisov and Stubbe*, 1997], it is also reasonable to suggest that only under conditions of energetic precipitation, such as would be expected from substorm activity, would the amplitude of the resulting Alfvén wave be large enough to be detectable by the spacecraft some 2500 km further out along the geomagnetic field line.

[32] The artificial generation of ULF waves and their subsequent injection into the magnetosphere is an important technique since it provides a means of investigating the naturally occurring processes which exist in the auroral acceleration regions. These form a very active area of research at present. Any disturbance in the lower ionospheric plasma localized a few km across the geomagnetic field and exhibiting time variations with scale times of seconds to tenths of seconds could launch field-guided ULF waves which would produce accelerating parallel electric fields when they reached the IAR boundary. This clearly indicates that a powerful feedback process could take place where precipitated electrons could enhance the original ionospheric disturbance, which would in turn increase the upgoing wave amplitudes. Although the trajectory of the resulting Alfvén waves may be restricted to a few Earth radii by the existence of ion gyroharmonic resonances along the path, the electrons accelerated upwards out of the IAR could, in principle, travel unimpeded for large distances out along field lines. This implies that it may be possible to tag field lines by detecting these electrons with satellites orbiting at several Earth radii.

5. Summary

[33] This study provides a detailed discussion on a new and innovative technique, first reported by *Robinson et al.* [2000], designed to tag a narrow flux tube traversed by orbiting spacecraft. It has been developed from the desire to be able to accurately compare observations of phenomena detected simultaneously in the ionosphere and in space. Until now inaccuracies in magnetospheric mapping have led to errors in the locations of common spatial features. The employment of a high power heating facility such as that which forms part of the EISCAT site in Tromsø, Norway is ideally suited to taking advantage of this method. By modulating the conductivity in the auroral electrojet, it has the ability to probe the magnetosphere, potentially out to great distances, by the use of field-guided Alfvén waves and their associated electron signatures.

[34] The observations presented here indicate that the ionospheric Alfvén resonator is a key element in the application of this technique for diagnosing the magnetosphere to distances of several Earth radii along the geomagnetic field line. As a result of the height profile of the Alfvén speed of the wave, which defines the upper boundary of the resonator, the polarization of the electric field associated with the wave rotates such that there is a significant field-parallel component. The amplitude of this parallel electric field maximizes near the boundary of the IAR. This region then acts to accelerate electrons along field lines in both directions. In principle these particles could be driven to great distances along the field line, where they may be detected by spacecraft with appropriate instruments on board. Testing this hypothesis is the aim of an ongoing experimental program. Both the FAST and Cluster spacecraft are being used to observe the accelerated electrons both below and above the boundary of the IAR. In addition, the expected deployment of the SPEAR active radar in 2003 will provide an opportunity to undertake these experiments on open field lines. The ability to sound the polar cap and cusp magnetospheres will be important in an area of solar-terrestrial physics, which is the focus of so much attention at present.

[35] **Acknowledgments.** The authors would like to thank the staff at the EISCAT site in Ramfjordmoen, Norway, the personnel in the EISCAT group at the Rutherford Appleton Laboratory, UK, for their assistance in organizing the experimental campaigns and subsequently with data analysis, and the team responsible for the operation of the FAST mission. Thanks are also due to the Finnish Meteorological Institute in Helsinki, Finland for providing data from the IMAGE magnetometer chain and to Tilmann Bösinger at the University of Oulu, Finland for making available data from the Kilpisjärvi Pulsation magnetometer.

References

Barton, C. E., et al., International geomagnetic reference field, 1995 revision presented by IAGA Division V, Working Group 8, *Phys. Earth Planet. Inter.*, *97*, 23, 1996.

Borisov, N., and P. Stubbe, Excitation of longitudinal (field-aligned) currents by modulated HF heating of the ionosphere, *J. Atmos. Sol. Terr. Phys.*, *59*, 1973, 1997.

Boteler, D. H., and R. J. Pirjola, The complex-image method for calculating the magnetic and electric fields produced at the surface of the Earth by the auroral electrojet, *Geophys. J. Int.*, *132*, 31, 1998.

Brekke, A., and J. Moen, Observations of high latitude ionospheric conductances, *J. Atmos. Terr. Phys.*, *55*, 1493, 1993.

Carlson, C. W., R. F. Pfaff, and J. G. Watzin, The Fast Auroral SnapshoT (FAST) mission, *Geophys. Res. Lett.*, *25*, 2013, 1998.

Cash, S. R., J. A. Davies, E. Kolesnikova, T. R. Robinson, D. M. Wright, T. K. Yeoman, and R. J. Strangeway, Electron acceleration observed by the FAST satellite within the IAR during a 3 Hz modulated EISCAT heater experiment, *Ann. Geophys.*, *20*, 1499, 2002.

Clemmow, P. C., and J. P. Dougherty, *Electrodynamics of Particles and Plasmas*, Addison-Wesley-Longman, Reading, Mass., 1969.

Davies, J. A., and M. Lester, The relationship between electric fields, conductances and currents in the high-latitude ionosphere: A statistical study using EISCAT data, *Ann. Geophys.*, *17*, 43, 1999.

Hughes, W. J., and D. J. Southwood, The screening of micropulsation signals by the atmosphere and ionosphere, *J. Geophys. Res.*, *81*, 3234, 1976.

James, H. G., R. L. Dowden, M. T. Rietveld, P. Stubbe, and H. Kopka, Simultaneous observations of ELF waves from an artificially modulated auroral electrojet in space and on the ground, *J. Geophys. Res.*, *89*, 1655, 1984.

James, H. G., U. S. Inan, and M. T. Rietveld, Observations on the DE1 spacecraft of ELF/VLF waves generated by an ionospheric heater, *J. Geophys. Res.*, *95*, 12,187, 1990.

Kimura, I., P. Stubbe, M. T. Rietveld, R. Barr, K. Ishida, Y. Kasahara, S. Yagitani, and I. Nagano, Collaborative experiment by Akebono satellite, Tromsø ionospheric heater, and European incoherent scatter radar, *Radio Sci.*, *29*, 23, 1994.

Kolesnikova, E., T. R. Robinson, J. A. Davies, D. M. Wright, and M. Lester, Excitation of Alfvèn waves by modulated HF heating of the ionosphere, with application to FAST observations, *Ann. Geophys.*, *20*, 57, 2002.

Landau, L. D., and E. M. Lifshitz, *Electrodynamics of Continuous Media*, Pergamon, New York, 1960.

Lester, M., W. J. Hughes, and H. J. Singer, Polarization patterns of Pi2 magnetic pulsations and the substorm current wedge, *J. Geophys. Res.*, *88*, 7958, 1983.

Lester, M., J. A. Davies, and T. S. Virdi, High-latitude Hall and Pedersen conductances during substorm activity in the SUNDIAL-ATLAS campaign, *J. Geophys. Res.*, *101*, 26,719, 1996.

Lühr, H., The IMAGE magnetometer network, *STEP Int. Newsl.*, *4*, 4, 1994.

Lysak, R. L., Generalised model of the ionospheric Alfvén resonator, in *Auroral Plasma Dynamics*, edited by R. L. Lysak, pp. 121–128, AGU, Washington, D. C., 1993.

Rietveld, M. T., H. Kohl, H. Kopka, and P. Stubbe, Introduction to ionospheric heating at Tromsø, 1, Experimental overview, *J. Atmos. Terr. Phys.*, *55*, 577, 1993.

Rishbeth, H., and A. P. van Eyken, EISCAT: Early history and the first ten years of operation, *J. Atmos. Terr. Phys.*, *55*, 525, 1993.

Rishbeth, H., and P. J. S. Williams, The EISCAT ionospheric radar: The system and its early results, *Q. J. R. Astron. Soc.*, *26*, 478, 1985.

Robinson, T. R., et al., FAST observations of ULF waves injected into the magnetosphere by means of modulated RF heating of the auroral electrojet, *Geophys. Res. Lett.*, *27*, 3165, 2000.

St.-Maurice, J.-P., and W. B. Hanson, Ion frictional heating at high latitudes and its possible use for an in situ determination of neutral thermospheric winds and temperatures, *J. Geophys. Res.*, *87*, 7580, 1982.

Stubbe, P., Review of ionospheric modification experiments at Tromsø, *J. Atmos. Terr. Phys.*, *58*, 349, 1996.

Stubbe, P., and H. Kopka, Modulated heating of the polar electrojet by powerful HF waves, *J. Geophys. Res.*, *82*, 2319, 1977.

Stubbe, P., and H. Kopka, Generation of Pc5 pulsations by polar electrojet modulation: First experimental evidence, *J. Geophys. Res.*, *86*, 1606, 1981.

Stubbe, P., H. Kopka, and R. L. Dowden, Generation of ELF and VLF waves by polar electrojet modulation: Experimental results, *J. Geophys. Res.*, *86*, 9073, 1981.

Stubbe, P., et al., Ionospheric modification experiments in northern Scandinavia, *J. Atmos. Terr. Phys.*, *44*, 1025, 1982.

Stubbe, P., et al., Ionospheric modification experiments with the Tromsø heating facility, *J. Atmos. Terr. Phys.*, *47*, 1051, 1985.

Wright, D. M., et al., Space Plasma Exploration by Active Radar (SPEAR): An overview of a future radar facility, *Ann. Geophys.*, *18*, 1248, 2000.

C. W. Carlson, University of California, Berkeley, CA 94720, USA.

S. R. Cash, P. J. Chapman, J. A. Davies, E. Kolesnikova, M. Lester, T. R Robinson, D. M. Wright, and T. K. Yeoman, Department of Physics and Astronomy, University of Leicester, University Road, Leicester, LE1 7RH, UK. (Darren.Wright@ion.le.ac.uk)

R. B. Horne, British Antarctic Survey, Cambridge CB3 0ET, UK.

M. T. Rietveld, EISCAT, Ramfjordmoen N-9027, Norway.

R. J. Strangeway, University of California, Los Angeles, CA 90024-1567, USA.

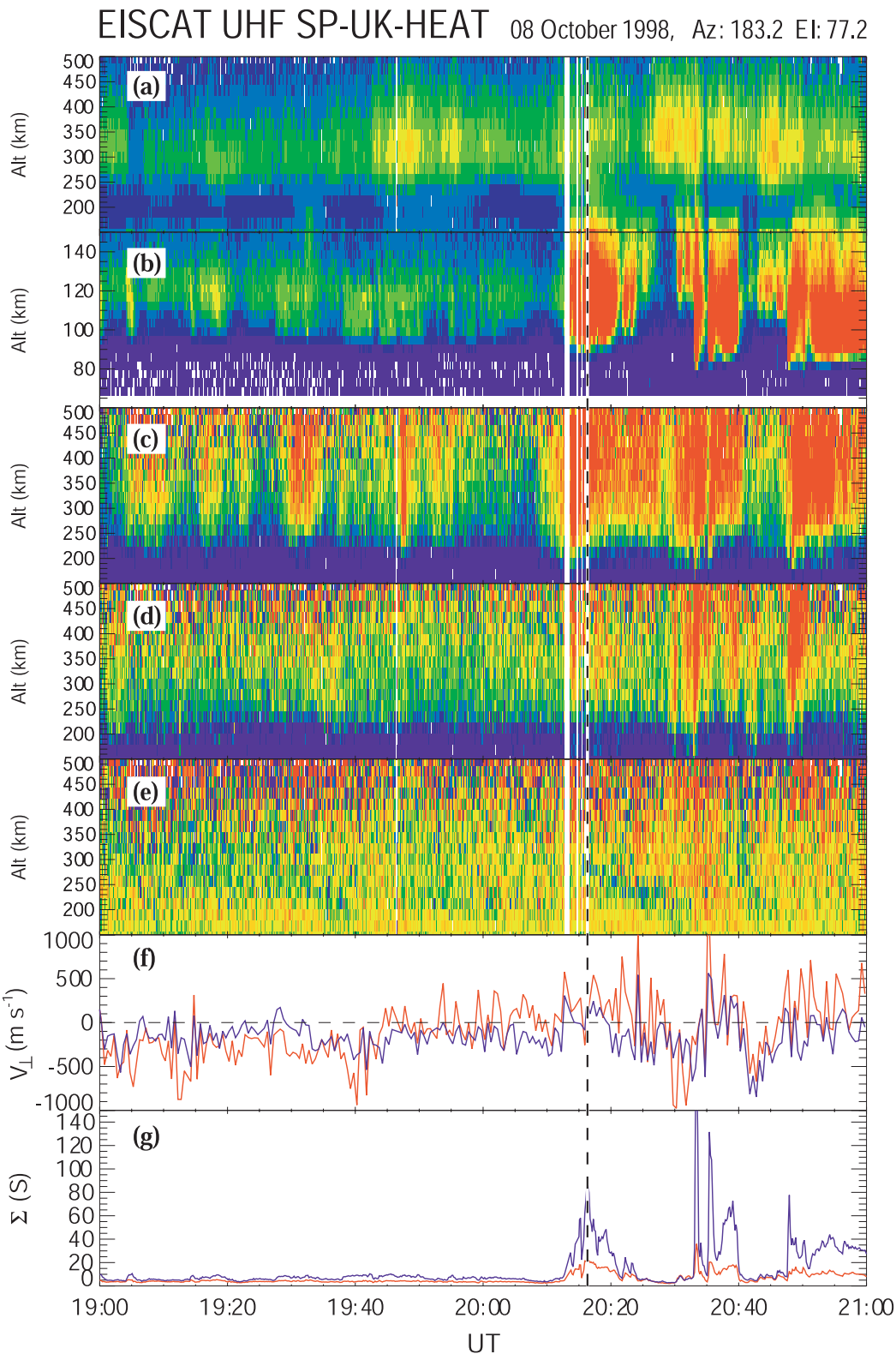

Figure 3. Data parameters measured by the EISCAT UHF radar during the run of SP-UK-HEAT on 8 October 1998. Plotted as a function of altitude along the field-aligned Tromsø beam (geographic azimuth: 183.2°, elevation: 77.2°) are: (a) *F* region electron density, (b) *D* and *E* region electron density derived from power profile, (c) *F* region electron temperature, (d) *F* region ion temperature and (e) *F* region line-of-sight ion velocity. Panel f illustrates the field-perpendicular eastward (red) and northward (blue) components of the ion velocity derived at the *F* region tristatic altitude of 250 km. Panel g, presents height-integrated Pedersen (red) and Hall (blue) conductivities. The dashed vertical line indicates the time at which FAST traversed the field line along which the UHF radar was observing.